Surface recombination measurements on III–V candidate materials for nanostructure light-emitting diodes

M. Boroditsky,[a] I. Gontijo, M. Jackson, R. Vrijen, and E. Yablonovitch[b]
University of California at Los Angeles, Los Angeles, California 90095

T. Krauss
Department of Electrical Engineering, Glasgow University, Glasgow, G12 8LT, United Kingdom

Chuan-Cheng Cheng and A. Scherer
California Institute of Technology, Pasadena, California 91125

R. Bhat
Bellcore, Corning, New York 14831

M. Krames
LumiLed, San Jose, California 95131

(Received 20 September 1999; accepted for publication 18 December 1999)

Surface recombination is an important characteristic of an optoelectronic material. Although surface recombination is a limiting factor for very small devices it has not been studied intensively. We have investigated surface recombination velocity on the exposed surfaces of the AlGaN, InGaAs, and InGaAlP material systems by using absolute photoluminescence quantum efficiency measurements. Two of these three material systems have low enough surface recombination velocity to be usable in nanoscale photonic crystal light-emitting diodes. © *2000 American Institute of Physics.*
[S0021-8979(00)01107-5]

INTRODUCTION

As the size of optoelectronic devices become smaller, surface effects begin to influence their performance. Surface recombination of carriers imposes limitations on the efficiency of nanocavity light-emitting diodes, vertical cavity surface emitting lasers with oxidized apertures, and other devices that require the size of the active region to be comparable to the minority carrier diffusion length. In this study we concentrated on surface characterization of different material systems and identification of those suitable for nanofabrication of active optoelectronic devices. This article is organized as follows: first we describe the experimental setup and the absolute calibration technique, then we introduce the recombination properties we are measuring or modeling. A radiative transport model based on the photon gas[1] approximation is used to extract internal quantum efficiency from the absolute photoluminescence measurements in the context of an $In_xGa_{1-x}N$ sample. The same model with slight modifications was used for two other systems: $In_{0.5}(Ga_{1-x}Al_x)_{0.5}P$ and $In_{0.53}Ga_{0.47}As$. Gallium nitride and chemically passivated InGaAs will be shown to possess a relatively low surface recombination velocity (on the order of 1×10^4 cm/s) while the InGaAlP material system has surface recombination velocity an order of magnitude higher. We also show that surface damage produced by chemically assisted ion beam etching can be cured by a gentle wet etching and chemical passivation.

EXPERIMENTAL SETUP

Surface recombination velocity was determined by absolute photoluminescence efficiency measurements, using a setup as shown in Fig. 1. Samples are optically pumped with an appropriate laser photon energy above the band gap. The absolute external quantum efficiency is calibrated by referencing the measured photoluminescence against the scattered light reading from a perfect white Lambertian reflector.[2] In this way, the collection cone solid angle of the photodetector is identical in both measurements. Corrections are made for different transmission through the optical setup and the detector quantum efficiency ratio at the photoluminescence and pump wavelengths. A simple radiative transport model[3] is used to obtain the internal quantum efficiency of the active material from the measured external quantum efficiency. Furthermore, comparison of the internal quantum efficiency from double heterostructure samples against that from the samples with an exposed active region provides information on the surface recombination velocity of the exposed surfaces.

RADIATIVE TRANSPORT MODEL

We begin with some definitions:

(1) External quantum efficiency η_{ext} is defined as a ratio of the number of photoluminescence (PL) photons coming out of the sample to the number of photons absorbed in the sample. This is a quantity we can measure.

(2) Internal radiative quantum efficiency η_{int} is the probability that an electron–hole pair created in the active region will recombine radiatively. Internal quantum efficiency is a figure-of-merit for an optoelectronic material.

---

[a]Present address: AT&T Labs, Red Bank, NJ 07701.
[b]Author to whom correspondence should be addressed; electronic mail: eliy@ee.ucla.edu

 © 2000 American Institute of Physics

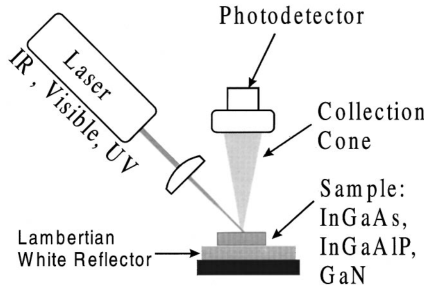

FIG. 1. Experimental setup for photoluminescence measurements. The absolute external quantum efficiency is measured by calibrating the measured photoluminescence from the sample against the reading measured from the laser scattered off a perfect white Lambertian reflector. The collection cone is the same for both measurements, so that only a correction for the system wavelength dependence of detector quantum efficiency has to be taken into account.

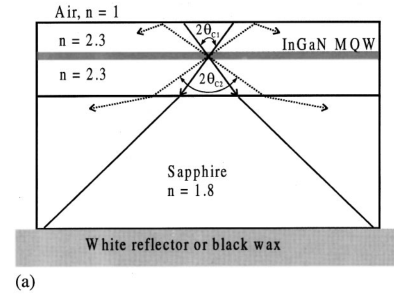

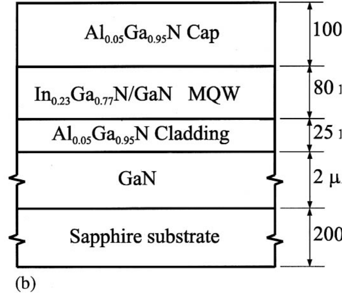

FIG. 2. (a) The semiconductor structure corresponding to the radiative transport model consists of a thin semiconductor film sitting on a sapphire substrate. (b) The schematics of the AlGaN/InGaN MQW structure grown by MOCVD on a *C*-plane sapphire substrate.

(3) Light extraction efficiency $\eta_{\mathrm{extraction}}$ is a fraction of internally generated PL photons that manage to escape from the sample. It depends strongly on the geometry of the sample. It also depends on the internal quantum efficiency if reabsorption in the active region has to be taken into account. For certain simple geometries, light extraction efficiency can be easily calculated.

(4) Finally, if optical pumping creates electron–hole pairs outside of the active region, we define collection efficiency η_{coll} as a fraction of carriers that diffuse to the active region. If all carriers are collected in the active region, $\eta_{\mathrm{coll}}=1$.

Combining all these definitions, external quantum efficiency can be expressed in terms of the three other quantities, which can be measured or calculated:

$$\eta_{\mathrm{external}}=\eta_{\mathrm{coll}}\eta_{\mathrm{int}}\eta_{\mathrm{extract}}. \tag{1}$$

Initially we will describe a radiative transport model used to calculate internal quantum efficiency in GaN. (For InGaAlP and InGaAs the models employed are almost identical, except they take into account the samples' structure such as an absorbing substrate in the case of InGaAlP.) As can be seen from Fig. 2(a), the InGaN model considers a film of GaN (refractive index $n_{\mathrm{GaN}}=2.3$) grown on the sapphire substrate with refractive index $n_{\mathrm{S}}=1.8$. There are two critical angles and two escape cones associated with them: total internal reflection at the semiconductor–air interface $\theta_{C1}=\arcsin(1/n_{\mathrm{GaN}})$ and at the semiconductor–sapphire interface $\theta_{C2}=\arcsin(n_{\mathrm{S}}/n_{\mathrm{GaN}})$. We employ geometrical optics to calculate escape and reabsorption probabilities. Spontaneous emission is assumed to have an isotropic angular distribution. Since the GaN film is relatively thick compared to the wavelength of light in the material [see Fig. 2(b)], a statistical ray optics model[1] is justified and the calculation of emission into individual electromagnetic modes[4] is not necessary.

Suppose N_{inc} photons are incident on the sample. $N_{\mathrm{inc}}T_{\mathrm{inc}}$ electron–hole pairs are created in the cap layer of the sample, where T_{inc} is the Fresnel transmission for the incident wave. $N_1=N_{\mathrm{inc}}T_{\mathrm{inc}}\eta_{\mathrm{coll}}$ of them will reach the active region. If the material internal efficiency is η_{int}, then $\eta_{\mathrm{int}}N_1$ photons are emitted, $E\eta_{\mathrm{int}}N_1$ photons escape, and $Z\eta_{\mathrm{int}}N_1$ photons are reabsorbed, where E is the escape probability of an emitted photon and Z is the reabsorption probability. Then the reabsorbed photons are reemitted in the amount $Z\eta_{\mathrm{int}}^2N_1$. Absorption and reemission continues leading to a number of escaped photons N_{esc} gives by the sum of a geometric series

$$N_{\mathrm{esc}}=E\eta_{\mathrm{int}}N_1+E\eta_{\mathrm{int}}(Z\eta_{\mathrm{int}}N_1)+E\eta_{\mathrm{int}}(Z\eta_{\mathrm{int}})(Z\eta_{\mathrm{int}}N_1)+\ldots=\frac{E\eta_{\mathrm{int}}N_1}{1-Z\eta_{\mathrm{int}}}. \tag{2}$$

It is clear from Eq. (2) that reabsorption plays a significant role only if internal quantum efficiency is high.

Keeping in mind that external quantum efficiency η_{ext}, the quantity that we measure, is the ratio of the number of escaped photons to the number of photons incident on the sample, i.e., $\eta_{\mathrm{ext}}=N_{\mathrm{esc}}/N_{\mathrm{inc}}$, we can invert Eq. (2) and solve it for internal quantum efficiency η_{int}

$$\eta_{\mathrm{int}}=\frac{(\eta_{\mathrm{ext}}/ET_{\mathrm{inc}})}{\eta_{\mathrm{coll}}+Z(\eta_{\mathrm{ext}}/ET_{\mathrm{inc}})}. \tag{3}$$

The escape probability E is given by the Fresnel transmission probability $T(\theta)$ integrated over the escape cone solid angle and divided by 4π sr

$$E=\frac{1}{4\pi}\int_0^{2\pi}d\varphi\int_0^{\theta_{C_1}}T(\theta)\sin\,\theta\,d\theta\cong\frac{\langle T\rangle}{4n_{\mathrm{GaN}}^2}\approx 0.07, \tag{4}$$

where $\langle T\rangle$ stands for the transmission coefficient averaged over the escape cone. Now we will address the reabsorption probability Z.

The diameter of the pump laser beam is about 50 μm, which is much larger than the InGaN/GaN film thickness (≈ 2 μm) and both are much thinner than the sapphire sub-

strate. We will assume that photons reabsorbed outside of the optically pumped region are reemitted very inefficiently, due to the resulting low carrier concentration np. Therefore, reabsorption and reemission are important only for photons bouncing inside the thin InGaN film, while photons reflected from the bottom sapphire surface are negligibly recycled. Then the fraction Z of reabsorbed photons becomes the sum of three terms

$$Z=\frac{1}{4\pi}\left[\int_0^{2\pi}d\varphi\int_0^{\theta_{C_1}}(1-e^{-\alpha d/\cos\theta})R(\theta)\sin\theta\,d\theta+\int_0^{2\pi}d\varphi\int_{\theta_{C_1}}^{\theta_{C_2}}(1-e^{-\alpha d/\cos\theta})\sin\theta\,d\theta+\int_0^{2\pi}d\varphi\int_{\theta_{C_2}}^{\pi-\theta_{C_2}}\sin\theta\,d\theta\right] \quad (5)$$

representing three cone angle zones $0\rightarrow\theta_{C_1}$, $\theta_{C_1}\rightarrow\theta_{C_2}$, and $\theta_{C_2}\rightarrow(\pi-\theta_{C_2})$. The photons beyond $(\pi-\theta_{C_2})$ transmit to the bottom of the sapphire substrate and are assumed not to contribute to the remission and not to reach the photodetector. In Eq. (5), $R(\theta)$ is the polarization-averaged reflectivity of the GaN–air interface, α is the reabsorption coefficient of the active region material at the photoluminescence wavelength, and d is the overall thickness of the absorbing quantum wells. The first term in Eq. (5) describes the reabsorption within the θ_{C_1} inner escape cone. The second term corresponds to reabsorption of photons emitted within the second escape cone θ_{C_2} but outside the first. These photons cross the active region once before they go into the substrate. The third term refers to reabsorption of totally internally reflected light in the semiconductor film. This last term dominates reabsorption and is simply $\sqrt{1-n_S^2/n_{GaN}^2}\cong 0.62\approx Z$, while the two other terms are merely corrections. In this analysis we have assumed that light reflected from the sapphire–air interface is reabsorbed outside of the optically pumped region and does not contribute efficiently to further photoluminescence.

There is a problem with Eq. (3), since the η_{coll} on the right hand side is not exactly known, but is surely less than 1. Therefore Eq. (3) gives a lower limit to η_{int}

$$\eta_{int}\geqslant\frac{(\eta_{ext}/ET_{inc})}{1+Z(\eta_{ext}/ET_{inc})}. \quad (6)$$

Likewise, Eq. (3) can be solved for the collection efficiency η_{coll}

$$\eta_{coll}=\frac{(\eta_{ext}/ET_{inc})(1-Z\eta_{int})}{\eta_{int}}. \quad (7)$$

Once again, η_{int} on the right hand side of Eq. (7) is not exactly known, but it is surely less than 1. Therefore we can use Eq. (7) to place a lower limit on carrier collection efficiency

$$\eta_{coll}\geqslant(\eta_{ext}/ET_{inc})(1-Z). \quad (8)$$

Thus a measurement of η_{ext} can place at a lower limit on η_{int} through Eq. (6) and a lower limit on η_{coll} through Eq. (8). This procedure will be useful if the experimental results for η_{ext} points to limits on η_{int} and η_{coll} that are reasonably close to 1. For InGaN, for example, the limits will be shown to be $0.87<\eta_{int}<1$ and $0.87<\eta_{coll}<1$, constraining the experimental values very tightly.

GALLIUM NITRIDE

The InGaN multiple quantum well (MQW) structure schematically shown in Fig. 2(b) was grown using metalorganic chemical vapor deposition (MOCVD) on a C-plane sapphire substrate.[5] It was optically pumped using the 325 nm line of a continuous wave HeCd laser.[2] The lower limit on internal quantum efficiency η_{int} measured and analyzed by Eq. (6) ranges from 40% to 87% for various samples. Variation in the sample quality was correlated with the number of quantum wells in the InGaN MQW region and was not attributed to the properties of the GaN cap layer. Such high internal quantum efficiencies allowed us to calculate the upper limit on the surface recombination at the GaN surface using the considerations below.

The optical absorption length for the 325 nm wavelength in the GaN cap layer is only 80 nm,[6] which is comparable to the cap layer thickness $L_{cap}=100$ nm. Therefore the pump light is absorbed everywhere throughout the cap layer of the GaN, and the electron–hole pairs generated near this surface need to diffuse into the MQW region, as shown in Fig. 2(b), to contribute to photoluminescence. Since the observed collection efficiency η_{coll} is quite good, the diffusion length L_D in GaN must be greater than the cap thickness $L_{cap}=100$ nm. The solution of the diffusion equation in this case provides an upper limit on collection efficiency

$$\eta_{coll}\leqslant\frac{D/L_{Cap}}{D/L_{Cap}+S}+\frac{S}{D/L_{Cap}+S}\left(\frac{1}{\alpha L_{Cap}}-\frac{1}{e^{\alpha L_{Cap}}-1}\right), \quad (9)$$

where S is the surface recombination velocity and D is the ambipolar diffusion constant, the diffusion constant of the slower species, which are holes. Inverting Eq. (9) yields an upper limit on the surface recombination velocity in $Al_{0.05}Ga_{0.95}N$, which is $S<0.3D/L\sim3\times10^4$ cm/s with the diffusion constant assumed[7] to be 1 cm^2/s in undoped $Al_{0.05}Ga_{0.95}N$.

We also made a measurement of the sample with the 300 nm thick cap layer and the same quantum well (QW). In this case the absorption length was smaller than the cap thickness, that is $\alpha L_{Cap}\gg1$, and the last term in Eq. (9) becomes small. The expression for the collection efficiency becomes simpler, corresponding to having all carriers generated at the surface (see Appendix)

$$\eta_{Coll}\leqslant\frac{D/L_{Cap}}{D/L_{Cap}+S}. \quad (10)$$

The value for surface recombination velocity obtained from this measurement with the same assumption was $S=2.8\times10^4$ cm/s, in good agreement with the previous result.

The optical model described above neglects reflections from the bottom surface of the sapphire substrate since most of those photons are reflected and absorbed outside of the

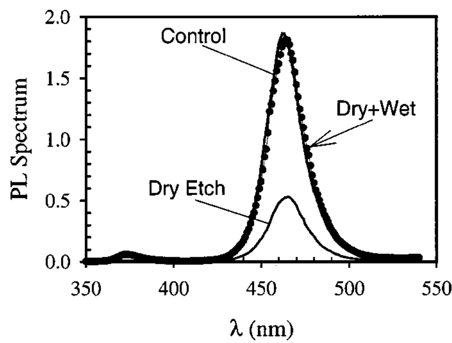

FIG. 3. Dry etching produces good surface morphology but causes damage which reduces drastically the material photoluminescence efficiency. This can be recovered by a subsequent 5 s KOH:H_2O (0.04 M) wet-etching step that removes the damage.

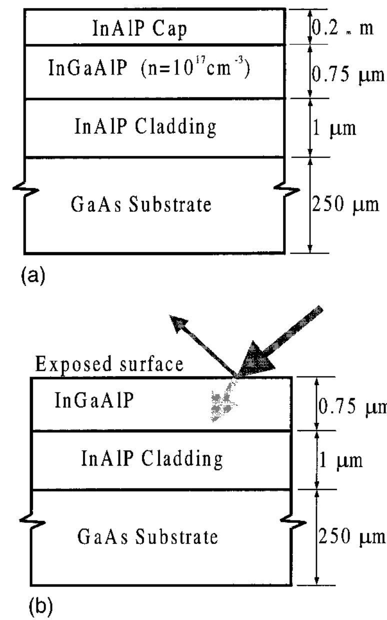

FIG. 4. (a) The InGaAlP sample consists of 0.75 μm thick $In_{0.5}(Ga_{0.92}Al_{0.08})_{0.5}P$ ($\lambda=630$ nm) active region doped at the $n=10^{17}$ cm^{-3} level sandwiched between n-type InAlP cladding layers grown on absorbing GaAs substrate. (b) When the top InAlP cladding layer is etched away, the nonradiative surface recombination on the exposed surface of the active region becomes the dominant recombination process.

optically pumped region, and cannot be re-emitted. The pump level for these experiments was 10 mW onto a 50 μm diam spot, or $\sim$500 W/cm^2. At lower pumping intensities the internal PL efficiency goes down, due to the requirement of a high np product to generate high efficiency. Therefore absorption and emission outside of the pumped region is inefficient and can be neglected.

Fabrication of nanoscale devices often involves dry etching. However, as is the case with GaAs and InP compounds, we found that the dry etching process leaves a damaged GaN surface, which increases the surface recombination velocity. In our experiment, the PL of an ''as-grown'' GaN sample was first measured to determine the internal quantum efficiency and the surface recombination velocity (SRV), which was found to be $S=2.8\times10^4$ cm/s. The sample was then etched in a chemically assisted ion beam etching machine for 1 min in $Ar^+ + Cl_2$, which removed 30 nm from the top cap layer. Figure 3 shows that after etching, the integrated PL from the sample dropped by a factor of 3.5, and SRV increased to $S=7\times10^4$ cm/s. However, a gentle wet etching[8] in KOH:H_2O (0.04 M) for 5 s resulted in a dramatic recovery of the PL efficiency, with a consequent decrease in the surface recombination velocity, back to $S=2.9\times10^4$ cm/s, as shown in Fig. 3. It is interesting that the wet etching depth was only 5–10 nm of material, which indicates that the damage introduced by the dry etching step is very shallow, allowing it to be effectively removed.

InGaAlP

In this case we studied samples consisting of a 0.75 μm thick $In_{0.5}(Ga_{1-x}Al_x)_{0.5}P$ ($\lambda=630$ nm) active region doped at $n=10^{17}$ cm^{-3} level sandwiched between n-type InAlP cladding layers grown on an absorbing GaAs substrate [Fig. 4(a)]. The sample was optically pumped with the cw 568 nm argon–krypton laser, which is not absorbed by the InAlP cladding layer. This isotype double heterostructure allowed us to be unconcerned about p-n junction effects. Internal quantum efficiency of the as-grown double heterostructure sample was measured to be 80%. After the top cladding was removed with a H_3PO_4:H_2O:H_2O (5:1:1) etching solution as shown in Fig. 4(b), the surface of the active region was exposed to air. The PL signal, and hence internal quantum efficiency, dropped by a factor of 30. Since the thickness of the active region is less than the typical diffusion length in this material system, and there is a potential barrier at the substrate side of the active layer, the carrier density distribution is constant, even though electron–hole generation occurs mostly at the top interface (see Appendix). For that reason internal quantum efficiency of an as-grown structure and a structure with an exposed active region is simply determined by competition between the radiative and nonradiative recombination rates. The efficiency of the intact double heterostructure is

$$\eta_{\text{as-grown}}=\frac{1/\tau_R}{1/\tau_{NR}+1/\tau_R}, \tag{11}$$

and the efficiency when the InAlP cap of the double heterostructure is etched away is

$$\eta_{\text{etched}}=\frac{1/\tau_R}{1/\tau_{NR}+1/\tau_R+S/L}, \tag{12}$$

where τ_R and τ_{NR} are radiative and nonradiative minority carrier lifetimes and L is the thickness of the active region. We can estimate the surface recombination velocity from the doping level of the active region $N_D=10^{17}$ cm^{-3} and a typical value of the radiative recombination constant[9] $B\sim4\times10^{-10}$ cm^3/s using Eq. (11). The recombination rates would be $1/\tau_R=BN_D=4\times10^7$ s^{-1}, $1/\tau_{NR}=10^7$ s^{-1}. The surface recombination velocity is easily obtained from Eq. (12) and equals $S=10^5$ cm/s. This is about twice the surface recombination velocity previously reported for InGaP.[10] Surface treatment with ammonium sulfide used in Ref. 10 did not show any increase in PL signal. The poor surface prop-

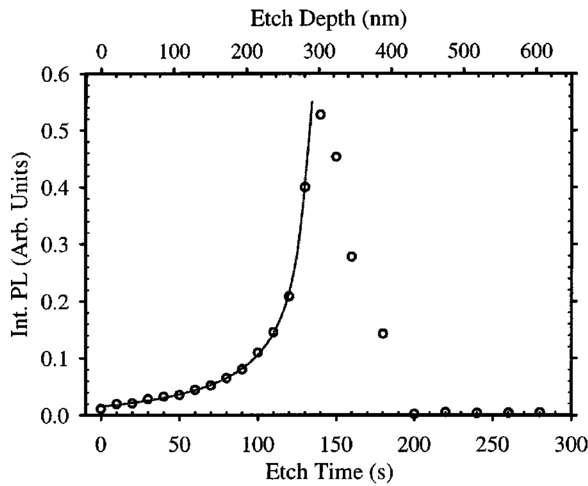

FIG. 5. Dependence of PL signal from the InGaAlP sample on the etch depth. The experimental data are shown with open circles. The signal increases as the cap layer gets thinner, and drops when the active layer becomes exposed. The solid line represents the fit obtained from solving the diffusion equation.

erties could be attributed to the presence of aluminum and its oxidation. The measured surface recombination velocity, although significantly higher than in GaN, is still an order of magnitude lower than that of an AlGaAs surface. Still there is a chance that some chemical treatment or regrowth technique might be established for the InGaAlP material system. In our PL measurements on the exposed active region, the surface degraded during a 30 s interval under an 8 mW laser beam focused to a 50 μm diam spot. Every time the laser beam was moved to a new location on the sample, the PL refreshed, and then decayed again. At lower pump power, the surface degraded more slowly. This observation suggests the possibility of sealing or passivation of the surface before it oxidizes.

We have also used an ultraviolet laser emitting at 325 nm to measure the surface recombination velocity in the $In_{0.5}Al_{0.5}P$ cap layer. Unlike the experiments with the Kr–Ar laser, the pump light in this case is absorbed in the top $In_{0.5}Al_{0.5}P$ layer. The absorption length at the 325 nm wavelength[11] is only 13 nm and thus the carrier photogeneration occurs in a very thin layer close to the sample surface. An absolute external quantum efficiency measurement was performed on the ''as-grown'' sample, using a setup similar to that described in Fig. 1. The sample was then etched in a solution of H_3PO_4:H_2O_2:H_2O (5:1:1), with an etch rate of 2.2 nm/s and the PL efficiency as a function of remaining cap thickness was plotted. At first we saw a large increase in the external PL emitted by the sample, until we reached an etch depth of about 280 nm. This happened because the carrier generation region was getting closer to the potential well. For larger etch depths, the PL dropped rapidly and stabilized at a very low level, below that of the ''as-grown'' sample, as shown with open circles in Fig. 5. The rapid decrease corresponds to the complete removal of the top InAlP cap layer, when the active region becomes exposed to air.[12] This introduces a large defect density, increasing the nonradiative recombination rate.

The increase in PL as the etch depth increases from 0 to 280 nm, just prior to the exposure of the active region, is explained by considering all the possible recombination channels for the photogenerated carrier concentration. The distribution of carriers with depth z, measured from the sample surface, obeys the diffusion equation and can be written as

$$n(z)=\frac{n_0}{\sinh(L/L_D)}\cdot\sinh\left(\frac{L-z}{L_D}\right), \tag{13}$$

where n_0 is the carrier concentration at the surface $(z=0)$, L is the thickness of the InAlP layer, and L_D is the carrier diffusion length. If P denotes the total carrier concentration generated per area per time, the carriers will recombine according to

$$P=S\cdot n(z)|_{z=0}+\int_0^L\frac{n(z)}{\tau}dz-D\left.\frac{\partial n}{\partial z}\right|_{z=L}, \tag{14}$$

where S is the surface recombination velocity of the InAlP cap layer, D is the ambipolar diffusion coefficient and τ is the carrier lifetime. The first term in Eq. (14) describes the fraction of carriers that recombine at the surface. The second term accounts for recombination in the InAlP layer and the third one represents the fraction of carriers collected by the active region. The collection efficiency η_{coll} is the ratio of the last term and the total recombination rate P

$$\eta=-\frac{D}{P}\left.\frac{\partial n}{\partial z}\right|_{z=L}. \tag{15}$$

After algebraic manipulations, Eqs. (14) and (15) result in a simple expression for the collection efficiency η_{coll}

$$\eta_{coll}=\left[\frac{SL_D}{D}\cdot\sinh(L/L_D)+\cosh(L/L_D)\right]^{-1}. \tag{16}$$

The first 14 points in Fig. 5 correspond to thinning down the cap layer, and can be used to extract L_D and *S/D* by fitting Eq. (16) to them. The fitted curve is plotted as a solid line in Fig. 5. The values obtained for the fitting parameters were $L_D=131.3$ nm and $S/D=0.098$ nm^{-1}. The diffusion length resulting from the fitting is small, corresponding to a lifetime of only $\tau=L_D^2/D=173$ ps, where a diffusion coefficient of $D=1$ cm^2/s was assumed. Using this same value of D in conjunction with the *S/D* value obtained above, a surface recombination velocity $S=9.8\times10^5$ cm/s is obtained. This is a factor of 10 higher than the surface recombination velocity obtained for the active region, which is probably related to the 50% aluminum concentration in the InAlP cladding layer.

InGaAs

Surface recombination velocity was also studied on a 20 nm n-type $In_{0.53}Ga_{0.47}As$ single QW structure with InP cladding layers grown on an InP substrate and separated from the substrate by an undoped 1 μm InGaAs etch-stop layer as shown in Fig. 6(a). The QW donor impurity concentration was $n\sim10^{18}$ cm^{-3}. This structure was designed for the fabrication of a thin-film cavity-enhanced light-emitting diode, a

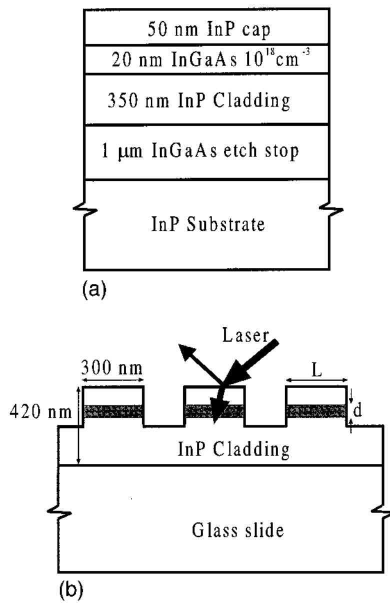

FIG. 6. (a) An n-type $In_{0.53}Ga_{0.47}As$ single quantum well structure with InP cladding layers was grown on a InP substrate and separated from the substrate by an undoped InGaAs etch-stop layer. (b) A set of mesas of widths ranging from 0.12 to 2 μm was etched so that the edges of the active region were exposed. The structure was bonded to a glass slide after the substrate removal process.

process that involves making an array of holes in the QW structure and bonding it onto a glass slide.[13] We are interested in measurements of surface recombination velocity on the vertical walls produced by chemically assisted ion beam etching (CAIBE) and in finding chemical treatments in order to minimize it. A set of mesas with widths ranging from 0.12 to 2 μm was etched as shown in Fig. 6(b) so that the active region edges were exposed. The overall double heterostructure was bonded to a glass slide prior to a total substrate removal process, as shown in Fig. 6(b). Internal quantum efficiency of the as-grown double heterostructure sample was nearly 100%. The ratio of the photoluminescence from the mesa etched sample to the PL signal from the intact double heterostructure depends on the surface recombination velocity and the width of the mesa. As in the $In_{0.5}(Ga_{1-x}Al_x)P$ case, the width of all mesas was smaller than a diffusion length, and the carrier density was uniform across the mesa. In this case the expression for quantum efficiency of the etched samples is very similar to that used for InGaAlP

$$\eta_{\text{int}}=\frac{1/\tau_R}{1/\tau_R+2S/w}, \tag{17}$$

where w is the mesa width. The factor of 2 in the denominator comes from two exposed surfaces instead of one for the InGaAlP case. Also, we neglected bulk nonradiative recombination since the PL measurements of the unetched material showed internal quantum efficiency close to 100%. Equation (17) can be transformed into

$$\frac{1}{\eta_{\text{int}}}=1+2S\tau_R\frac{1}{w}, \tag{18}$$

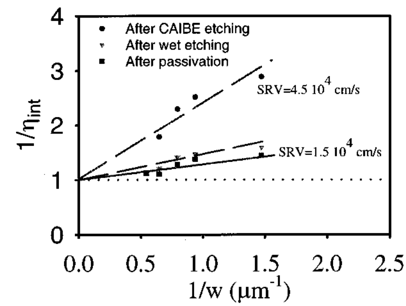

FIG. 7. Inverse quantum efficiency plotted vs inverse mesa width. The slope of the fitted lines are equal to $2S\tau_R$.

so that slope of the straight line $1/\eta$ vs $1/w$ gives the value of $2S\tau_R$ as shown in Fig. 7. The value of the relative constant B, assumed to be the same as in the InGaAlP case, was used to calculate τ_R, leaving S as the only adjustable parameter. A surface recombination velocity $S=4.5\times10^4$ cm/s was obtained by fitting Eq. (18) to the data for the mesas etched using the CAIBE technique (shown in circles in Fig. 7). After the surface damage was removed using the gentle wet etch in H_2SO_4:H_2O_2:H_2O (1:8:5000) solution (triangles in Fig. 7) SRV decreased to $S=1.7\times10^4$ cm/s. Further improvement was observed after a 5 min long passivation in a solution of ammonium sulfide $(NH_4)_2S$ (squares, SRV$=1.5\times10^4$ cm/s). It turned out that surface damage depends on the ion energy of the etching process. The reported results correspond to 500 V Ar^+ accelerating potential in the CAIBE process. The ion damage seems to be significantly deeper when 1500 V voltage is employed, resulting in larger surface recombination velocities and requiring more intensive cleaning.

SUMMARY OF MATERIAL PROPERTIES

In this article we studied surface recombination velocities in InGaN, InGaAlP, InAlP, and InGaAs material systems using absolute calibration photoluminescence measurements. The surface recombination velocity is shown to be $<3\times10^4$ cm/s on GaN, $<1.5\times10^4$ cm/s on passivated InGaAs, $\sim10^5$ cm/s on $In_{0.5}(Ga_{0.9}Al_{0.1})_{0.5}P$, and $\sim10^6$ cm/s on $In_{0.5}Al_{0.5}P$. We also showed that residual surface damage caused by dry etching could be removed by proper surface treatment. These results suggested that InGaAs and GaN are the most favorable material systems for nanofabrication of active devices based on photonic crystals.

We have also studied the ion damage produced during ion-beam etching. For GaN, it was found that the surface recombination velocity increased by a factor of 3.5 after removal by dry etching of 30 nm from the top layer. However, a gentle wet etching in KOH:H_2O (0.04 M) for 5 s resulted in a dramatic recovery of the PL efficiency, with a consequent decrease in the surface recombination velocity, back to its original value.

It is interesting that a similar effect was obtained for the InGaAs material. The dry etching step produced shallow damage, resulting in a surface recombination velocity increase by a factor of 3. A wet etching step in a H_2SO_4:H_2O_2:H_2O (1:8:5000) solution, performed after the

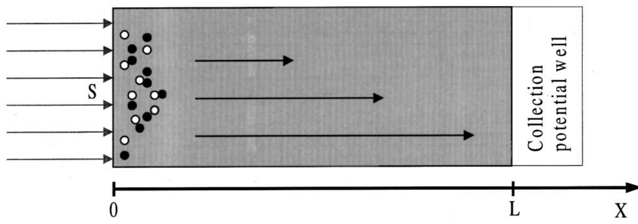

FIG. 8. The carriers are generated close to the surface with surface recombination velocity S and diffuse towards the potential well. The corresponding carrier density profiles are in Fig. 9. The light rays are indicated by the arrows from the left.

dry etching, resulted in a recovery of the PL efficiency and a reduction of the surface recombination velocity to its original value. Moreover, the ion damage depends on the ion energy of the etching process. As the accelerating potential in the dry-etching process is increased, more damage is produced, requiring a more intensive wet-etching cleaning.

APPENDIX: SOME SOLUTIONS OF THE DIFFUSION EQUATION

We list here some solutions of the steady state diffusion equation, that we used to model carrier distribution profile in two different configurations, which is given by

$$-D\nabla^2 n+\frac{n}{\tau}=G, \tag{A1}$$

where D is the ambipolar diffusion constant, τ is the carrier lifetime, and G is the volume carrier generation rate. In our experiments the carriers were generated by band-to-band absorption of incident light. In all our experiments the diffusion equation had to be solved in only one dimension. The presence of an open surface imposes the following boundary condition:

$$-D\frac{dn}{dx}=Sn, \tag{A2}$$

where S is called SRV, and is an important characteristic of a semiconductor surface or interface.

1. Injection on one side (Fig. 8)

We consider a case when the incident light with photon flux density J is all absorbed in the cap region and produces electron–hole pairs close to the cap surface characterized by the surface recombination velocity S. The generated carriers have to diffuse into the collection region as in Fig. 8. A situation like this took place in the GaN and $In_{0.5}Al_{0.5}P$ experiments with a thin cap layer. If the cap thickness is L, and the open surface is located at $x=0$, and the collecting potential well is at $x=L$, the boundary conditions are

$$-D\frac{dn(0)}{dx}=Sn(0)$$

and

$$n(L)=0. \tag{A3}$$

Collection efficiency η_{coll} is the fraction of the carriers that reach the collecting potential well. We define the diffusion length $L_D\equiv\sqrt{\tau D}$ and diffusion velocity $V_D\equiv\sqrt{D/\tau}$. Figure 9 summarizes carrier distribution profiles and collection efficiency dependence for four simple yet important cases.

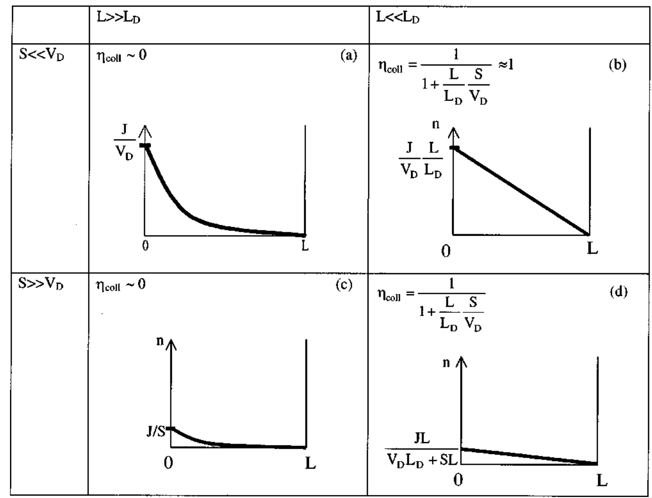

FIG. 9. Carrier distribution profiles $n(x)$ and collection efficiencies corresponding to the photon flux J absorbed close to the surface with surface recombination velocity S. The cap layer of thickness L is characterized by the carrier lifetime τ and diffusion constant D. We introduce a diffusion length $L_D=\sqrt{\tau D}$ and diffusion velocity $V_D=\sqrt{D/\tau}$. The vertical axes are marked with the carrier density for each case. (a), (b), (c), and (d) represent different combinations of diffusion lengths and surface recombination velocities. The top left corner of each square gives a formula for η_{coll}, the efficiency in each case.

When the cap is thick, $L\gg L_D$, as in cases (a) and (c), the collection efficiency is exponentially small, because most of the carriers recombine inside the cap or at the surface. If the surface recombination rate is small [case (a)], that is $S<V_D$, the carriers recombine in the volume. In the presence of fast surface recombination [case (c)], most of the carriers recombine at the surface and the rest in the volume of the cap layer.

The situation changes if the cap layer is thinner than the diffusion length, $L\ll L_D$ [cases (b) and (d)]. The solution of the diffusion equation is a straight line, and the recombination loss is negligible in the bulk of the cap. If the surface recombination is small, as in case (b), the collection efficiency approaches 100%. In the opposite case of strong SRV, the collection efficiency is

$$\eta_{\text{coll}}=\frac{1}{1+\frac{L}{L_D}\frac{S}{V_D}}. \tag{A4}$$

As can be seen from the four cases in Fig. 9, a high collection efficiency requires both a low surface recombination velocity and a thin cap layer.

2. Uniform injection (Fig. 10)

We consider the case when the incident light with uniform photon flux density J is absorbed throughout an active area, providing a uniform volume carrier generation rate G, as shown in Fig. 10. The photoinduced electron–hole pairs can either recombine nonradiatively at the exposed surfaces

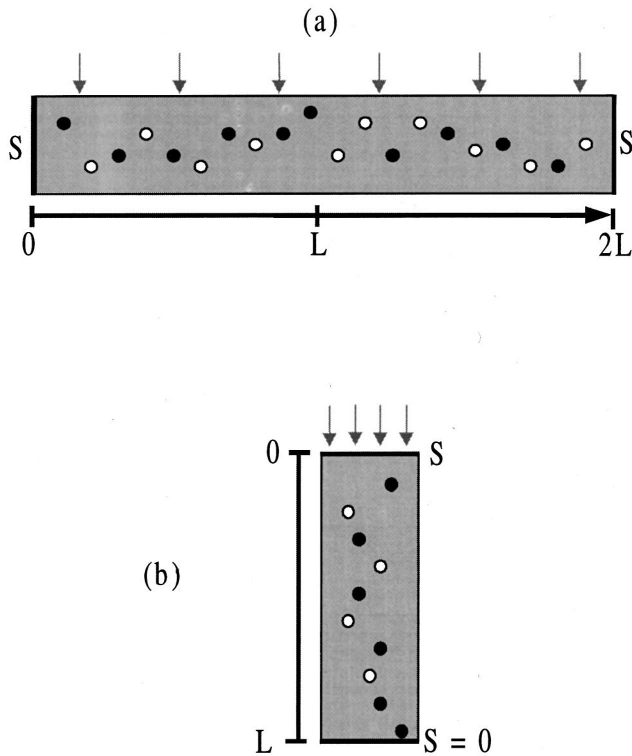

FIG. 10. Carriers are injected uniformly, and can either recombine radiatively in the volume or nonradiatively at the surfaces. The corresponding carrier density profiles are in Fig. 11. In the InGaAlP experiments, the single sided pump radiation came from the top, but was weakly absorbed throughout the thickness *L*. This vertical geometry has the identical diffusion equation solution as in (a).

characterized by the surface recombination velocity *S* or radiatively within the active area. In the experiment on the exposed surface of InGaAlP, the single-sided pump radiation came from the top, but was weakly absorbed in the layer of thickness *L*. The diffusion constant is *D* and the radiative recombination lifetime in the active region is τ. As before, we define the diffusion length $L_D \equiv \sqrt{\tau D}$ and diffusion velocity $V_D \equiv \sqrt{D/\tau}$. The figure of merit in this case is the internal quantum efficiency η_{int}, defined as the fraction of carriers that recombine radiatively. The carrier flux is zero at $x=L$, since in both cases [Figs. 10(a) and 10(b)] there is no density gradient and the secondary boundary condition is simply

$$D\frac{dn(L)}{dx}=0. \tag{A5}$$

The carrier distribution profiles and corresponding internal quantum efficiencies are summarized in Fig. 11, which considers four different cases depending on the relation between L and L_D and S and V_D.

If $L \gg L_D$ [Figs. 11(a) and 11(c)], only a small fraction of the active region near the edge is affected by surface recombination. Thus most of the recombination occurs radiatively in the active region and, almost independently of the SRV,

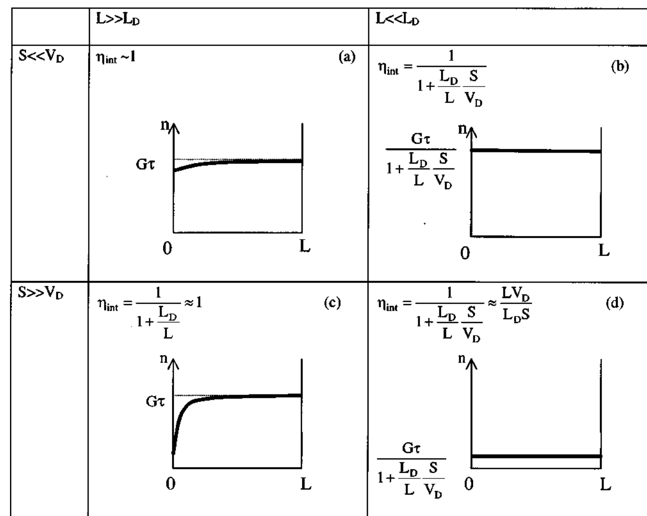

FIG. 11. Carrier distribution profiles $n(x)$ and internal efficiencies corresponding to the flux *J* absorbed uniformly in an active region with a single-side open surface having surface recombination velocity *S*. The active region of width *2L* or depth *L* corresponding to Figs. 3(a) and 3(b) is characterized by the carrier lifetime τ and diffusion constant *D*. The denominator in (b) can also be written as $(1+S\tau/L)$.

the internal quantum efficiency is close to 100%. The generation rate per unit volume is *G* and the carrier density is close to $G\tau$.

However, in most nanostructured materials, the diffusion length is larger than the dimensions of the active region, $L \ll L_D$ as in Figs. 11(b) and 11(d). In that situation, the internal efficiency might be high only if the surface recombination velocity is small, $S \ll V_D$, as shown for Fig. 11(b). All results in Fig. 11 can be readily used for the case with two open surfaces, Fig. 10(a), e.g., the InGaAs experiment.

[1] E. Yablonovitch, J. Opt. Soc. Am. **72**, 899 (1982).
[2] C. Reese, M. Boroditsky, E. Yablonovitch, S. Keller, B. Keller, and S. DenBaars, 1996-CLEO Conference, Technical Digest, Anaheim, CA, 1996, p. 141.
[3] M. Boroditsky, R. Ragan, and E. Yablonovitch, Sol. Energy Mater. Sol. Cells **57**, 1 (1999).
[4] H. R. Stuart and D. G. Hall, J. Opt. Soc. Am. A **14**, 3001 (1997).
[5] S. Keller, B. Keller, H. Maui, D. Kapolnek, A. Abare, U. Mishra, L. Coldren, and S. DenBaars, International Symposium on Blue Lasers and Light Emitting Diodes, Chiba University, Chiba, Japan, 1996.
[6] J. F. Muth, J. H. Lee, I. K. Shmagin, R. M. Kolbas, H. C. Casey, B. P. Keller, U. K. Mishra, and S. B. DenBaars, Appl. Phys. Lett. **71**, 2572 (1997); D. Brunner, H. Angerer, E. Brustarret, F. Freudenberg, R. Hopler, R. Dimitrov, O. Ambacher, and M. Stutzmann, J. Appl. Phys. **82**, 5090 (1997).
[7] I. Eliashevich, Y. Li, A. Osinsky, C. Tran, M. Brown, and R. Karlicek, Proc. SPIE **3621**, 28 (1999).
[8] C. Youtsey, I. Adesida, and G. Bulman, Appl. Phys. Lett. **71**, 2151 (1997).
[9] E. Yablonovitch, T. J. Gmitter, and R. Bhat, Phys. Rev. Lett. **61**, 2546 (1988).
[10] S. J. Pearton, F. Ren, W. S. Hobson, C. R. Abernathy, and U. K. Chakrabarti, Proc. IEEE , 186 (1994).
[11] H. Kato, S. Adachi, H. Nakanishi, and K. Ohtsuka, Jpn. J. Appl. Phys., Part 1 **33**, 186 (1994).
[12] E. Yablonovitch, H. M. Cox, and T. J. Gmitter, Appl. Phys. Lett. **52**, 1002 (1988).
[13] M. Boroditsky, R. Vrijen, T. F. Krauss, R. Coccioli, R. Bhat, and E. Yablonovitch, J. Lightwave Technol. **17**, 2096 (1999).